

Propagation of Avalanches in Mn_{12} -Acetate: Magnetic Deflagration

Yoko Suzuki,¹ M. P. Sarachik,¹ E. M. Chudnovsky,² S. McHugh,¹ R. Gonzalez-Rubio,¹ Nurit Avraham,³ Y. Myasoedov,³ E. Zeldov,³ H. Shtrikman,³ N. E. Chakov,⁴ and G. Christou⁴

¹*Department of Physics, City College of New York, CUNY, New York, New York 10031, USA*

²*Department of Physics and Astronomy, Lehman College, CUNY, Bronx, New York 10468-1589, USA*

³*Department of Condensed Matter Physics, The Weizmann Institute of Science, Rehovot 76100, Israel*

⁴*Department of Chemistry, University of Florida, Gainesville, Florida 32611, USA*

(Received 21 June 2005; published 30 September 2005)

Local time-resolved measurements of fast reversal of the magnetization of single crystals of Mn_{12} -acetate indicate that the magnetization avalanche spreads as a narrow interface that propagates through the crystal at a constant velocity that is roughly 2 orders of magnitude smaller than the speed of sound. We argue that this phenomenon is closely analogous to the propagation of a flame front (deflagration) through a flammable chemical substance.

DOI: [10.1103/PhysRevLett.95.147201](https://doi.org/10.1103/PhysRevLett.95.147201)

PACS numbers: 75.50.Xx, 75.60.Jk, 82.33.Vx

Mn_{12} -acetate (hereafter Mn_{12} -ac) is a prototypical molecular magnet composed of magnetic molecules, $[\text{Mn}_{12}\text{O}_{12}(\text{CH}_3\text{COO})_{16}(\text{H}_2\text{O})_4] \cdot 2\text{CH}_3\text{COOH} \cdot 4\text{H}_2\text{O}$, with cores consisting of 12 Mn atoms strongly coupled by exchange to form superparamagnetic clusters of spin $S = 10$ at low temperatures [1]. Arranged in a centered tetragonal lattice, the spin of the Mn_{12} clusters is subject to strong magnetic anisotropy along the symmetry axis (the c axis of the crystal). Below the blocking temperature of ≈ 3.5 K, the crystal exhibits remarkable staircase magnetic hysteresis due to resonant quantum spin tunneling between energy levels on opposite sides of the anisotropy barrier corresponding to different spin projections, as illustrated in Fig. 1(a) [2]. This and other interesting properties of Mn_{12} -ac have been intensively studied in the past decade (see Refs. [3–6] for reviews).

It has been known for some time [7] that Mn_{12} -ac crystals exhibit an abrupt reversal of their magnetic moment under certain conditions. This phenomenon, also observed in other molecular magnets, has been attributed to a thermal runaway (avalanche) in which the initial relaxation of the magnetization toward the direction of the field results in the release of heat that further accelerates the magnetic relaxation. Direct measurements of the heat emitted by Mn_{12} -ac crystals [8], as well as measurements of the magnetization reversal in pulsed magnetic fields [9], have confirmed the thermal nature of the avalanches. More recently, the electromagnetic signal associated with avalanches was detected [10,11], and it was argued that if the radiation is of thermal origin it would indicate a significant increase in the temperature of the crystal. This has not been confirmed by direct bulk measurements of the temperature using a thermometer. Evidence has been obtained [12] that the avalanche may not be a uniform process throughout the sample. No clear understanding of the avalanche process has emerged to date.

In this Letter we report local time-resolved measurements of fast magnetization reversal (avalanches) in

mm-size single crystals of Mn_{12} -ac. We show that a magnetic avalanche takes the form of a thin interface between regions of opposite magnetization which propagates throughout the crystal with a constant field-dependent speed ranging from 1 to 15 m/s. We demonstrate that this phenomenon is closely analogous to the propagation of a flame front (deflagration) through a flammable chemical substance.

Microscopic arrays of Hall bars were used to measure the magnetization of three single crystals of Mn_{12} -ac with dimensions: sample 1, $0.29 \times 0.29 \times 0.64$ mm³; sample 2, $0.28 \times 0.28 \times 1.44$ mm³; sample 3, $0.24 \times 0.24 \times 1.02$ mm³. Eleven Hall bars of dimensions 10×10 μm^2 with 30 μm intervals were used for sample 1, and 30×30 μm^2 with 130 μm intervals for samples 2 and 3.

Using an excitation current of 2 μA , the Hall bar signal was amplified by a factor of 1200, and detected and recorded by several digital scopes and a data acquisition card. In order to ensure proper synchronization, one channel of each scope was anchored to the same signal. The Hall sensor and amplifier introduced combined delays of up to 3 μs . A magnetic field was applied in the z direction along the crystal easy axis (see Fig. 1), lowering (raising)

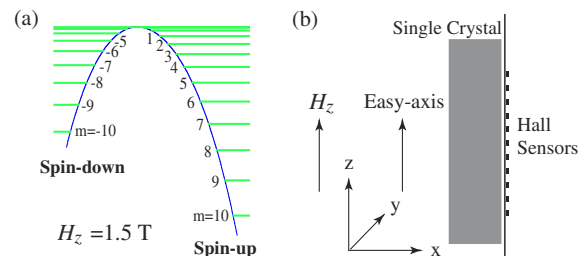


FIG. 1 (color online). (a) The potential energy function in a longitudinal magnetic field of 1.5 T. (b) Schematic diagram of a sample mounted on an array of Hall sensors used to detect B_x . Pronounced nonuniformity in magnetization during an avalanche generates large values of B_x .

the energy of the states corresponding to spin projections along (opposite to) the field direction. The Hall sensors were aligned to detect the magnetic induction of the sample in the x direction. B_x is proportional to the spatial derivative of M_z in the region near the sensor [13]. For a uniform magnetization in the z direction, B_x derives from the gradient at the sample ends, which is proportional to M_z itself. During an avalanche, there is a large contribution to B_x from the local region corresponding to the avalanche front, where $\partial M_z/\partial z$ is large.

The samples were immersed in liquid ^3He ; most of the data were obtained at the base temperature of 250 mK. The few points measured at 400 and 650 mK were found to lie on the same curve within the scatter of the data, indicating that the temperature dependence is weak. A longitudinal magnetic field (parallel to the easy axis) was swept back and forth through the hysteresis loop to ± 6 T until an avalanche was triggered. As reported in an earlier paper [14], avalanches occur in a stochastic way at 0.25 K both at resonant magnetic fields (where energy levels on opposite side of the barrier match; see Fig. 1) and away from resonance. Avalanches were also found for sample 2 for zero field-cooled conditions, where the sample starts from zero magnetization (instead of full saturation). In the experiments reported here, avalanches were invariably triggered at the top edge of a sample and traveled downward to the bottom edge.

Figure 2 shows an avalanche for sample 1. Steps due to quantum tunneling of the magnetization were observed, with a magnetization that was almost uniform throughout the sample, until an avalanche occurred, as shown in the inset. During the avalanche, the Hall bar recorded a large peak in B_x , signaling the abrupt onset of a highly nonuniform magnetization.

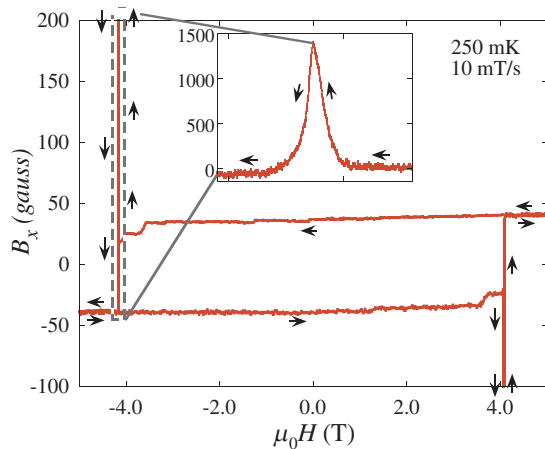


FIG. 2 (color online). Hysteresis loops for a single crystal of $\text{Mn}_{12}\text{-ac}$ (sample 1). B_x was recorded by a Hall sensor situated about $80 \mu\text{m}$ above the middle of the sample. Steps due to quantum tunneling of the magnetization are observed, as well as a sharp spike in B_x associated with an avalanche, shown in the inset.

For a field sweep rate of 10 mT/s and temperature 0.25 K, Fig. 3 shows an avalanche triggered at 4 T and recorded for sample 1 by seven of the 11 sensors placed in sequential positions near the center of the sample. The avalanche was triggered above the topmost sensor and traveled downward (see Fig. 1). B_x displays the largest peak at the center due to the finite size of the sample. The inset shows the sensor position as a function of the time at which the sensor registered the peak amplitude. The slope of the straight line drawn through these points yields a constant velocity of 12 m/s for this avalanche.

Figure 4 summarizes the data obtained for the velocity of propagation of avalanches recorded in different longitudinal magnetic fields for all three samples. For avalanches that change the full magnetization from one direction to the other ($\Delta M = 2M_{\text{sat}}$), the data for samples 2 and 3 lie on approximately the same curve. Smaller velocities are obtained for avalanches in sample 2 when starting from the zero-field-cooled condition ($\Delta M = M_{\text{sat}}$). Avalanches for sample 1 were obtained only at relatively high magnetic fields in the vicinity of 4 T; the velocities for this sample range in value and do not appear to be consistent with data for the other two samples. In all cases the velocity increases with increasing magnetic field.

Interestingly, as shown in Fig. 5, an approximate collapse is obtained for all the data when plotted as a function of $g\mu_B H S(\Delta M/M_{\text{sat}})$, the energy per molecule released during an avalanche. Thus, avalanches require the release of a threshold energy, above which they propagate with a speed that appears to be a linear function of the energy for the range investigated in these experiments.

We note that, from a thermodynamic point of view, a crystal of Mn_{12} molecules placed in a magnetic field

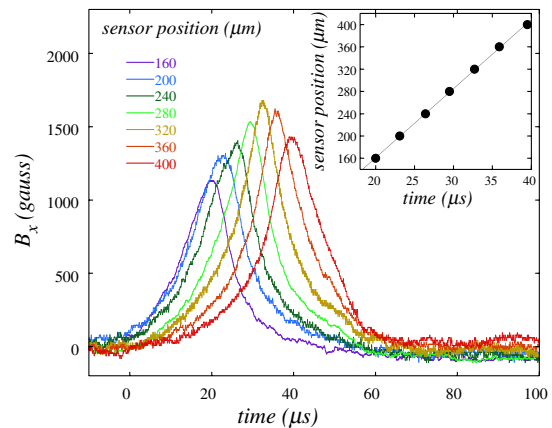


FIG. 3 (color online). Signals recorded by seven equally spaced Hall sensors situated near the center of sample 1 during an avalanche triggered at 4 T. The left (right) trace corresponds to the top (bottom) sensor (see Fig. 1). Sensor positions are measured relative to the top of the sample, with the center at $\approx 320 \mu\text{m}$. The inset shows sensor position versus the time at which the sensor recorded peak amplitude. A straight line fit yields a constant velocity of propagation of 12 m/s.

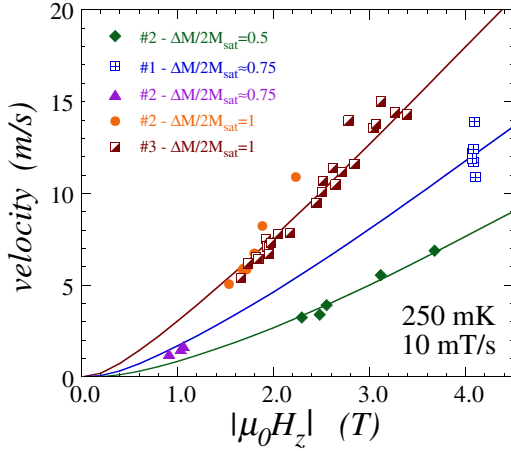


FIG. 4 (color online). Velocity of propagation of avalanches versus the magnetic field at which the avalanches occurred (samples are identified by number). ZFC denotes data obtained for the sample cooled in the absence of a magnetic field. From top to bottom, the curves are fits obtained for $\Delta M/2M_{\text{sat}} = 1, 0.75,$ and 0.5 (see text).

opposite to the magnetic moment is equivalent to a metastable (flammable) chemical substance. In our case, the role of the chemical energy stored in a molecule is played by the difference in the Zeeman energy, $\Delta E = 2g\mu_B HS$, for states of the $\text{Mn}_{12}\text{-ac}$ molecule that correspond to \mathbf{S} parallel and antiparallel to \mathbf{H} ; here $g = 1.94$ is the gyromagnetic factor and μ_B is the Bohr magneton. For $\text{Mn}_{12}\text{-ac}$ in a field of a few Tesla, ΔE is below 0.01 eV, as is the energy barrier, $U(H)$, between spin-up and spin-down states due to the magnetic anisotropy. Thus, for the avalanches in $\text{Mn}_{12}\text{-ac}$, ΔE and U are 2 orders of magnitude smaller than typical energies of chemical reactions. However, our temperature range is also more than 2 orders of magnitude below room temperature, making the analogy rather close.

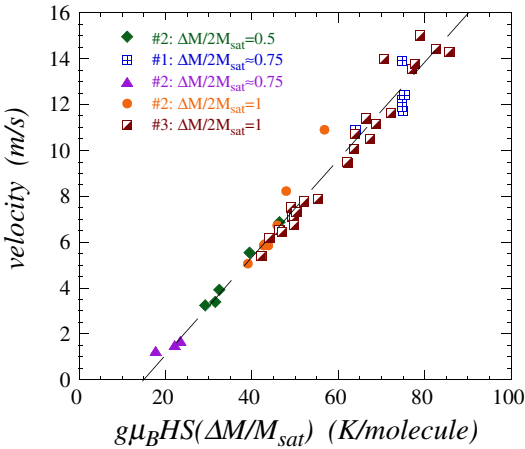


FIG. 5 (color online). Velocity of propagation of avalanches versus energy released per molecule. The line is drawn to guide the eye.

A well-known mechanism for the release of energy by a metastable chemical substance is combustion or slow burning, technically referred to as deflagration [15]. It occurs as a flame front of finite width, δ , propagates at a constant speed, v , small compared to the speed of sound. The parameter δ is determined by the distance, $\delta \sim \sqrt{\kappa\tau}$ through which the heat diffuses during the time of the “chemical reaction” τ . In our case

$$\tau(H) = \tau_0 \exp\left[\frac{U(H)}{k_B T_f}\right], \quad (1)$$

where $\tau_0 \sim 10^{-7}$ s is the attempt time [2] and T_f is the temperature of the flame. The dynamics of the flame are governed by the thermal diffusivity, κ , which obeys

$$\frac{\partial T}{\partial t} = \kappa \nabla^2 T. \quad (2)$$

For κ independent of T , substituting $T = T(x - vt)$ at $x > vt$, one obtains $T = T_f \exp[-v(x - vt)/\kappa]$ in front of the interface, which yields $v\delta = \kappa$. An interface thickness that is at most the distance between sensors, $\delta \sim 30 \mu\text{m}$, and the experimentally measured velocities of the order of 1–15 m/s, yield an upper bound on κ in the range 10^{-5} to 10^{-4} m²/s, consistent with heat pulse experiments [16].

Combining $v\delta = \kappa$ with $\delta \sim \sqrt{\kappa\tau}$, one obtains

$$v \sim \frac{\delta}{\tau} \sim \sqrt{\kappa/\tau} = \left(\frac{\kappa}{\tau_0}\right)^{1/2} \exp\left[-\frac{U(H)}{2k_B T_f}\right]. \quad (3)$$

The strongest dependence of v on H derives from the exponential, which contains the known dependence [17] of the energy barrier, $U(H)$, on the magnetic field. Using the measured phonon specific heat of $\text{Mn}_{12}\text{-ac}$ [18,19] and an approximate calculation for the magnetic contribution [18], we estimate that the released magnetic energy raises the temperature of the flame front to 10.5 K for an avalanche at 1 T and 14.7 K for an avalanche triggered at 4 T. Fits to Eq. (3) then yield the curves shown in Fig. 4, and reasonable values for κ and τ_0 [20]. Here we have used the simplest, rather crude model of deflagration, a widely studied phenomenon that is known to be quite complex [21]. A more complete theory is needed to account for the apparent data collapse of Fig. 5.

We have shown that fast magnetization reversal, or magnetic avalanches, require a threshold energy and proceed as a well defined front traveling at a subsonic velocity. These features are very similar to the propagation of a flame through a chemical substance. It is well known that deflagration of a flammable gas will not occur in a pipe of diameter, d , small compared to the width of the flame front, δ . In our case, unless δ is small compared to the crystal diameter, the heat generated will diffuse mostly through the sample walls and will not sustain the propagation of the interface. Indeed, avalanches tend to occur in larger crystals with sufficiently large magnetization opposite to the direction of the field. The latter corresponds to the condi-

tion of “flammability” [21] needed to provide sufficient heating (that is, the large T_f) required for $\delta < d$. It is interesting to note that the few avalanches recorded around 1 T did not result in full reversal of the magnetization. At these low fields the conditions for ignition are marginally satisfied, and the “flame” is extinguished before the process of magnetization reversal has been completed. In addition to available magnetic energy (flammability), the conditions for ignition may also depend on the shape and quality of the crystal, which may account for differences observed for different samples.

Slow burning at a subsonic speed (deflagration) is governed by the linear process of thermal conductivity. In addition to deflagration, unstable chemical substances also exhibit detonation, which can be caused by instability of the flame or by direct initiation other than through deflagration [21]. The initial stage of the detonation corresponds to a nonlinear supersonic shock wave [15,21]. Theory and experimental studies of advanced stages of detonation are lacking. Based on the close analogy between unstable chemical substances and molecular magnets, the latter may well exhibit “magnetic detonation” under the right conditions.

In conclusion, we have demonstrated that avalanches in the magnetization reversal of sufficiently large crystals of magnetic molecules are very similar to flame propagation (deflagration) through a metastable chemical substance. The analogy between the two systems derives from the magnetic bistability of molecular nanomagnets. Our observation of “magnetic deflagration” offers a potentially important new way to investigate the phenomenon of flame propagation (and possibly detonation). In contrast to deflagration in flammable chemical substances, the analogous process of “magnetic deflagration” in molecular nanomagnets is nondestructive, reversible, and much easier to control.

We are grateful to D. Graybill for participation in various aspects of this work and to K. M. Mertes, J. R. Friedman, M. Bal, and J. Tejada for valuable discussions. The work at City College was supported by NSF Grant No. DMR-0451605. Support was provided for EMC by NSF Grant No. EIA-0310517, and for GC by NSF Grant No. CHE-0071334. E.Z. acknowledges the support of the Israeli Science Foundation Center of Excellence.

-
- [1] R. Sessoli, D. Gatteschi, A. Caneschi, and M. A. Novak, *Nature (London)* **365**, 141 (1993).
 [2] J. R. Friedman, M. P. Sarachik, J. Tejada, and R. Ziolo, *Phys. Rev. Lett.* **76**, 3830 (1996).

- [3] B. Barbara, L. Thomas, F. Lioni, I. Chiorescu, and A. Sulpice, *J. Magn. Magn. Mater.* **200**, 167 (1999).
 [4] D. Gatteschi and R. Sessoli, *Angew. Chem., Int. Ed.* **42**, 268 (2003).
 [5] J. R. Friedman, in *Exploring the Quantum/Classical Frontier Recent Advances in Macroscopic Quantum Phenomena*, edited by J. R. Friedman and S. Han (Nova Science, Hauppauge, NY, 2003), p. 179.
 [6] E. del Barco, A. D. Kent, S. Hill, J. M. North, N. S. Dalal, E. Rumberger, D. N. Hendrickson, N. Chakov, and G. Christou, *J. Low Temp. Phys.* **140**, 119 (2005).
 [7] C. Paulsen and J.-G. Park, in *Quantum Tunneling of Magnetization-QTM'94*, edited by L. Gunther and B. Barbara (Kluwer, Dordrecht, The Netherlands, 1995), pp. 189–207.
 [8] F. Fominaya, J. Villain, P. Gandit, J. Chaussy, and A. Caneschi, *Phys. Rev. Lett.* **79**, 1126 (1997).
 [9] E. del Barco, J. M. Hernandez, M. Sales, J. Tejada, H. Rakoto, J. M. Broto, and E. M. Chudnovsky, *Phys. Rev. B* **60**, 11 898 (1999).
 [10] J. Tejada, E. M. Chudnovsky, J. M. Hernandez, and R. Amigo, *Appl. Phys. Lett.* **84**, 2373 (2004).
 [11] A. Hernandez-Minguez, A. Jordi, R. Amigo, A. Garcia-Santiago, J. M. Hernandez, and J. Tejada, *Europhys. Lett.* **69**, 270 (2005).
 [12] M. Bal, J. R. Friedman, K. M. Mertes, W. Chen, E. M. Rumberger, D. N. Hendrickson, N. Avraham, Y. Myasoedov, H. Shtrikman, and E. Zeldov, *Phys. Rev. B* **70**, 140403(R) (2004).
 [13] Nurit Avraham, Ady Stern, Yoko Suzuki, K. M. Mertes, M. P. Sarachik, E. Zeldov, Y. Myasoedov, H. Shtrikman, E. M. Rumberger, D. N. Hendrickson, N. E. Chakov, and G. Christou, *cond-mat/0505264* [*Phys. Rev. B* (to be published)].
 [14] Y. Suzuki, M. P. Sarachik, N. Avraham, Y. Myasoedov, H. Shtrikman, E. Zeldov, E. M. Rumberger, H. Hendrickson, and G. Christou, *J. Appl. Phys.* **97**, 10M517 (2005).
 [15] L. D. Landau and E. M. Lifshitz, *Fluid Dynamics* (Pergamon, New York, 1987).
 [16] J. Tejada (private communication). A 10 μ s heat pulse was found to travel a distance $d = 1$ mm in a time $t \sim 20$ –50 ms, yielding $\kappa \sim d^2/t \sim (2$ –5) $\times 10^{-5}$ m²/s.
 [17] Jonathan R. Friedman, *Phys. Rev. B* **57**, 10 291 (1998).
 [18] A. M. Gomes, M. A. Novak, R. Sessoli, A. Caneschi, and D. Gatteschi, *Phys. Rev. B* **57**, 5021 (1998); A. M. Gomes, M. A. Novak, W. C. Nunes, and R. E. Rapp, *J. Magn. Magn. Mater.* **226–230**, 2015 (2001).
 [19] F. Fominaya, J. Villain, T. Fournier, P. Gandit, J. Chaussy, A. Fort, and A. Caneschi, *Phys. Rev. B* **59**, 519 (1999).
 [20] The fitting procedure yielded prefactors of the exponential in Eq. (3) that differed by as much as a factor of 2 for different ΔM , reflecting the fact that the prefactor is not well known within the theory. On the other hand, the exponential dependence is well captured by the model.
 [21] I. Glassman, *Combustion* (Academic Press, New York, 1996).